Chapter

Wet and Dry Spells over Southeast Peninsular India

Mohana S. Thota

Abstract

The southeast peninsular India contains, to name a few, several important cities crucial for trade and economic growth of the country, rice bowls, institutes for science and technology, space port, etc. Despite its importance, not many reports exist on rainfall and its variation on different temporal scales over this region during southwest monsoon, partly because the rainfall in this region is relatively less and it forms only a minor part of all India rainfall. Here, an attempt has been made to understand differences in thermal and dynamical characteristics and energetics of the atmosphere between wet and dry spells of the Indian summer monsoon over the southeast India by utilizing various observations and reanalysis products. Observations demonstrate that the difference in the thermal structure between wet and dry spells is significant only in the lower troposphere (< 2-3 km) with mean CAPE values are reaching as much as 1000 Jkg-1during wet spell. Vertical buoyancy profiles indicate the bi-modal distribution during dry spells with peaks in 700 and 500 hPa levels. The observed thermal features are not confined to Gadanki but seen over entire southeast peninsular India. Associated dynamical variations also exhibit obvious differences during wet and dry spell. The diurnal variation of winds exhibits difference in amplitude and phase are remarkably large during dry spell than in wet spell. Synthesis are all the measurements indicates that the thermal and dynamical differences observed in wet and dry spells are pronounced in the boundary layer.

Keywords: wet and dry spells, Monsoon, CAPE, Southeast peninsular India

1. Introduction

The term “monsoon” is an Arabic word, which means seasonal reversal of wind direction. Prevailing wind direction between winter and summer seasons are the basis for delineation of the regional monsoon around the world. According to [1], the monsoonal region in the tropics extends between 25S–35N and 30 W–170E. This broad region comprises of three parts, the African monsoon and South and East Asian monsoon systems. From past several decades, these monsoon systems acquired fervent attention by scientific community and common people as well. These are globally distributed atmospheric phenomena giving surplus amount of water to mankind. It is estimated that the monsoon rains all over the world and provides ~60% of global water supply [2]. Among the monsoon systems over the globe, the Asian monsoon is the largest, and Asian regions are critically influenced by the evolution and inherent variability. It interacts with El Nino/Southern Oscillation and extratropical weather systems and thereby controls the global circulation through teleconnections. Further, monsoon variability is also influenced

by aerosols, tropical typhoon activity, etc. The Asian monsoon can be classified into two types: (1) South Asian monsoon or Indian monsoon, which affects the Indian subcontinent and surrounding regions and (2) East Asian monsoon which affects the countries like China, Korea, and Japan. In the present chapter, we primarily focus on the Indian monsoon especially over southeast India.

2. Indian monsoon: Southeast peninsular India

Indian subcontinent is situated at the vicinity of the monsoonal region defined by [1]. Copious amount of rainfall occurs over the Indian sector during June–September, also known as summer (or southwest) monsoon season. It accounts for ~75–80% of the annual rainfall over major parts of the Indian subcontinent. Agrarian countries like India heavily depend on this rainfall. Any deficit in the seasonal rainfall will have an adverse effect on the agriculture and economy of the country. The commencement of rainy season over Indian subcontinent is distinguished by the widespread rainfall over Kerala coast in late May/early June. In general monsoon sets over Kerala on June 1 with a standard deviation of 8 days [3]. Monsoon arrival to the central India takes 10–15 days after the onset and completely occupies the subcontinent by mid-July [15]. The withdrawal of monsoon takes place in September from northwest India, and by October 20, retreat of the southwest monsoon completes, and another monsoon, called northeast monsoon, sets in over southeast India.

Mean seasonal summer monsoon rainfall is not homogeneous (see **Figure 1**); it varies spatially (within India) and temporally (within the season) over the Indian region. From **Figure 1**, a large spatial asymmetry in seasonal mean rainfall can be seen over the Indian subcontinent. The rainfall occurrence is high over the West coast and Northeastern India (approx. >16 cm), moderate to heavy over central India (8–15 cm), and low over northwestern and southeastern peninsular India (~4 cm). Southeast peninsular India receives considerable amount of rainfall during the northeast monsoon season, i.e., from October

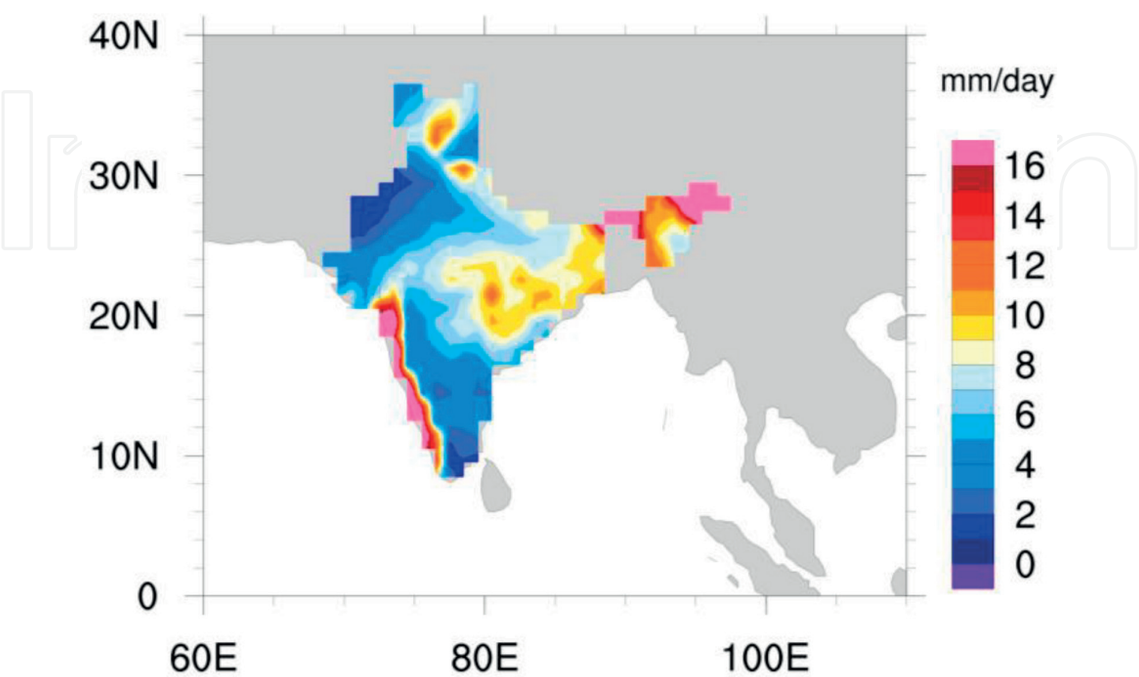

Figure 1.
Spatial distribution of mean seasonal summer monsoon rainfall. The high-resolution 1 × 1 degree rainfall data generated by IMD are used for this plot.

through December. After the onset of the southwest monsoon over Kerala coast, monsoon rainfall and the intertropical convergence zone (ITCZ) move northward. However, the northward propagation or advance of the monsoon is not always smooth; rather it takes place in pulses or epochs, in association with the convective activity [4].

During the southwest monsoon season, the large-scale rainfall distribution is mostly concentrated over two regimes: North Bay of Bengal and south of the equator in Indian Ocean. Winds converge in these regions, and these regions become most favored zones for convection and the formation of the tropical convergence zone (TCZ). Mean position of the TCZ is not constant; instead it oscillates with different periodicities and scales. Oscillations of the TCZ are synchronized with enhanced and suppressed convective activity known as active and break phases of the monsoon. Thus, the monsoon is a manifestation of the seasonal migration of the ITCZ, and monsoon variability is associated with the space–time variation of the ITCZ [5]. As discussed earlier, the seasonal monsoon rainfall varies spatially and temporally, and the variation of rainfall depends mainly on the duration and the time of occurrence of active and break phases. Natural disasters caused by the extreme hydrometeorological events are manifestation of intraseasonal variability (ISV) [6–8].

3. Intraseasonal variability

The day-to-day variability in the rainfall plays an important role in deciding the seasonal rainfall. Seasonal mean monsoon rainfall is affected by the occurrence and strength of the active and break spells [6]. It is well known from the earlier studies that the modes of 30–60 days and 10–20 days are most important in controlling the Indian summer monsoon rainfall (ISMR) [5, 9–13]. [14] studied the spatial variability of intraseasonal oscillations (ISOs) in deficit and excess monsoon years and demonstrated the dominance of 30–60 days over west coast and southeast region during the deficit monsoon year, while excess monsoon years are characterized by high-frequency synoptic (3–5 days) oscillations. Another important result obtained by them is the weakening of 30–60-day oscillation and strengthening of 10–20-day oscillation over central India and some parts of the west coast.

Active and break spells of Indian monsoon associated with intraseasonal oscillations (ISOs) need to be understood properly as they control the seasonal rainfall. It is noted by several researchers that excess monsoon rainfall years generally have more active spells and deficit monsoon rainfall years will have prolonged and/or more break spells (see [15–17]). A modest decrease in the monsoon rainfall (e.g., 10% of the long-term mean) significantly affects the food productivity (see [15, 18–21]). The knowledge of active and break spells on a regional scale is more crucial and important than all-India integrated active/break spells for agriculture and water management sectors. Therefore, the prediction of occurrence of active/break spell and their duration is much more important for the management of sowing and harvesting than the seasonal mean rainfall. In the recent past, several research works have been carried out to understand and identify the active and break spells over the Indian subcontinent using various parameters (see [5, 17, 22–28]. Since the definitions and techniques used by the aforementioned authors for the identification of active and break spells are different, the duration and occurrence of the spells in any monsoon season can be different [29]. For instance, [30] reported that there is hardly any overlap between the spells observed by them and those observed by [15]. Ramamurthy [23] identified breaks over monsoon zone using the rainfall data from 1888 to 1967 and inferred that according to his

criteria, there were no break days observed in 10 consecutive years. However, the study reported that the duration of break days varies from 3 to 15 days with 30% of the spells longer than or equal to 7 days.

4. Spatial variability of active and break spells

Earlier studies have shown that intraseasonal variations in rainfall are not coherent over the Indian region and the active/break spells of some subdivisions are in opposite phase with each other [16, 31, 32]. For instance, the spatial structures of the active/break spells are organized in such a way that southeast peninsular and northeastern parts of India exhibit an out-of-phase relation with the monsoon zone or central India. Also, rainfall increases near the foothills of the Himalayas, following the northward movement of monsoon trough, during break spells for the monsoon zone. Therefore, knowledge of active and break spells on a regional scale is important as different regions grow different crops and follow different practices.

In a study, [33] demonstrated that there exists large spatial variability in active and break spells using 58 years (1951–2007) of high-resolution (1° × 1°) rainfall data generated by the India Meteorological Department (IMD) [16]. They generated spatial maps for rainfall fraction (in terms of %) corresponding to break periods as defined by different criteria, discussed above [17, 25–27] (**Figure 2**). **Figure 3** shows that large rainfall fraction of ~20–40% occurs over southeast India during all-India break. The clear discrepancy in the rainfall distribution between these regions indicates the need for identifying active and break spells separately for the southeastern region of India.

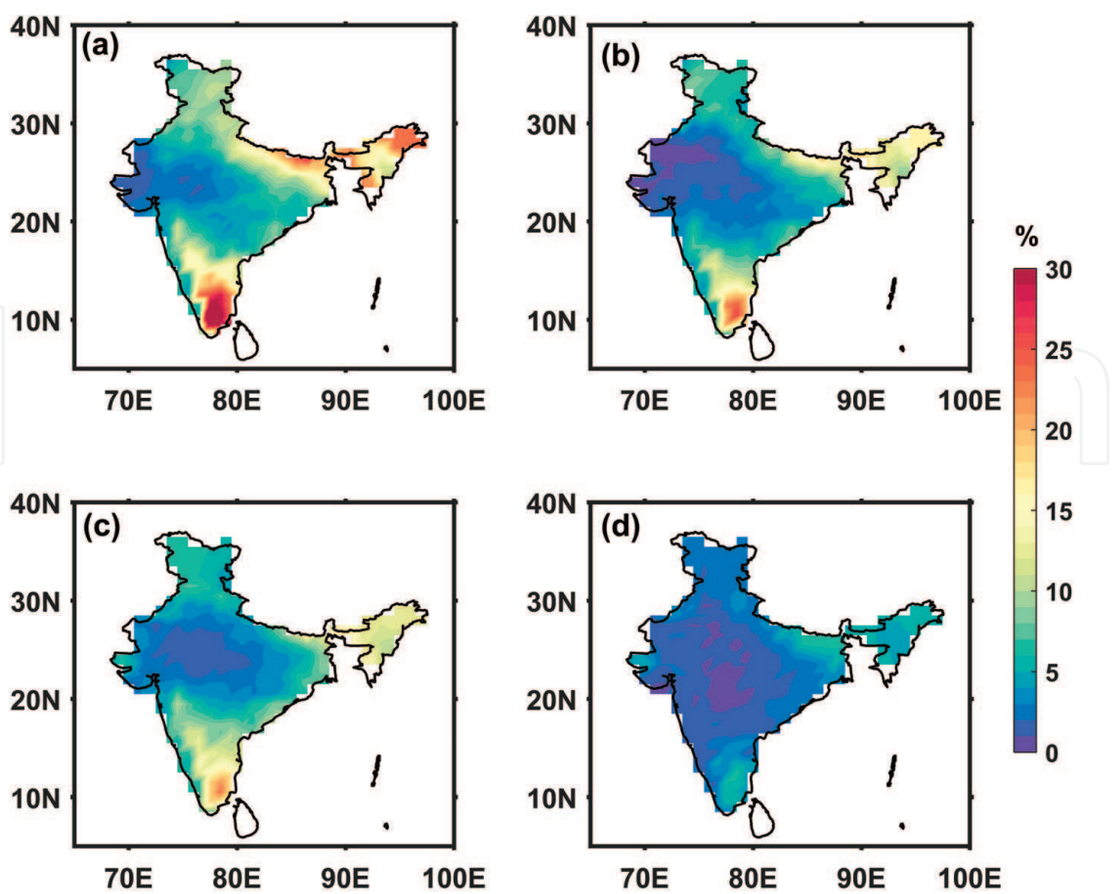

Figure 2.
Spatial distribution of rainfall fraction (%) in all-India break periods, as defined by (a) [25], (b) [27], (c) [17], and (d) [26]. Reproduced from ***Figure 1****, [33].*

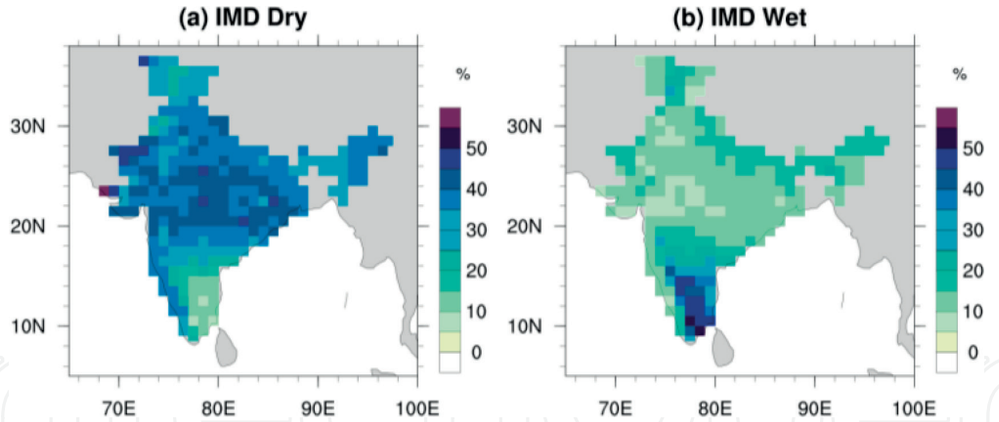

Figure 3.
Rainfall percentage contribution during (a) dry and (b) wet spells of the southwest monsoon from 1951 to 2015 using IMD 1 × 1 deg. gridded data.

4.1 Identification of wet and dry spells

In the present chapter, the terms "wet" and "dry" spells are used instead of active and break spells, in order to avoid confusion with all-India active and break spells of the summer monsoon rainfall. The method of analysis for the identification of wet and dry spells is discussed below. Wet and dry spells are identified using area-integrated surface rainfall measurements, following [16]. The area over which the surface rainfall is integrated (9.5°–15.5° N and 77.5°–81.5° E) is selected based on the correlation analysis. This is obtained by considering the correlation between time series of rainfall at each grid point and areal averaged rainfall. Only those grids with correlation coefficient >0.5 are considered. Following the procedure described in the above section, a total of 943 from 72 dry spells and 391 from 54 wet spells are identified from the 15 years (1995–2009). The spells are ranging from 5 to 50 days during dry and from 3 to 31 days during wet. Average time span during wet spell is ~7, whereas the span is ~13 days during the dry spell. Among dry (wet) spells, ~34 (48) % of spells have time span longer than the average length of dry (wet) spell.

It is general belief that the rainfall in the rain-shadow region of southeastern peninsular India occurs in isolated convective storms or along the coast mainly due to sea-breeze intrusions. To examine how much rainfall is due to large-scale systems (in wet spell) and how much is due to isolated storms (in dry spell), the rain amount contribution by each spell to the seasonal rainfall is estimated (**Figure 3**).

As mentioned above, the wet and dry spells are in opposite phase in the monsoon zone and southeast peninsular India, i.e., during wet spell, southeastern peninsular India gets good amount of rainfall; nevertheless the monsoon zone seldom gets rainfall and vice versa. Though the wet spell persists only 22% of time in the southwest monsoon, 50–60% of the seasonal rainfall occurs in that spell. On the other hand, only 5–20% of seasonal rainfall occurs in the dry spell. One can see clearly that good amount of rainfall (**Figure 3b**) occurs along the west coast in dry spell and almost no rain in the eastern side of the Western Ghats in the southern peninsula (south of 15° N) in wet spell.

5. Salient features of wet and dry spells

To know the basic differences between these wet and dry spells, it is necessary to understand the thermal and dynamical characteristics associated with these spells. To better understand these processes, observational data collected with

a suite of unique instruments at the National Atmospheric Research Laboratory (NARL), Gadanki (13.45 N, 79.2E), located over Southeast India is utilized. It is a semiarid region located in a complex hilly terrain at 375 m above mean sea level (MSL).

In the following subsections, a brief description of the basic characteristics of wet and dry spells is given. For those who are interested can find enough evidence and description in the research papers referenced therein.

5.1 Thermal characteristics

A comprehensive analysis is performed onto the radiosonde data launched from Gadanki twice daily during synoptic hours (00 GMT and 12 GMT) along with surface automatic weather station (AWS) data which has revealed several interesting facts during these spells. Majority of the soundings (~96%) reached above tropopause level and encouraged us to study the vertical variations of temperature (T) and moisture (q).

Figure 4 shows the variations of surface T and q between wet and dry spells are in the form of histograms (in terms of % occurrence). It is apparent from the figure that the wet spells are relatively moist and cooler than dry spells. Although the surface T and q distribution in these spells show some overlapping, the mean (mode) values differ by 1.6 K (~2 K) in T and ~2 g kg^{-1} in q. Note that the variations in T and q are not biased by the seasonal variations in T and q over the study region; rather, their difference in spells are mainly caused by the active/subdued convection in the monsoon season.

Next, to understand how convection in wet spells changes the vertical structure of thermodynamic variables through complex feedbacks (latent heating, etc.), the difference between wet and dry spells of composites of T ($T = Td - Tw$), q ($q = qd - qw$), and equivalent potential temperature, θe ($\Delta\theta e = \theta ed - \theta ew$), is given in **Figure 5**. Suffixes "d" and "w" denote dry and wet spells, respectively.

Maximum temperature differences are seen in the lower and upper troposphere and are of the order of 1–2 K. The lower troposphere (below ~2 km) and upper troposphere (11–16 km) are warmer in dry spell than in wet spell. Between

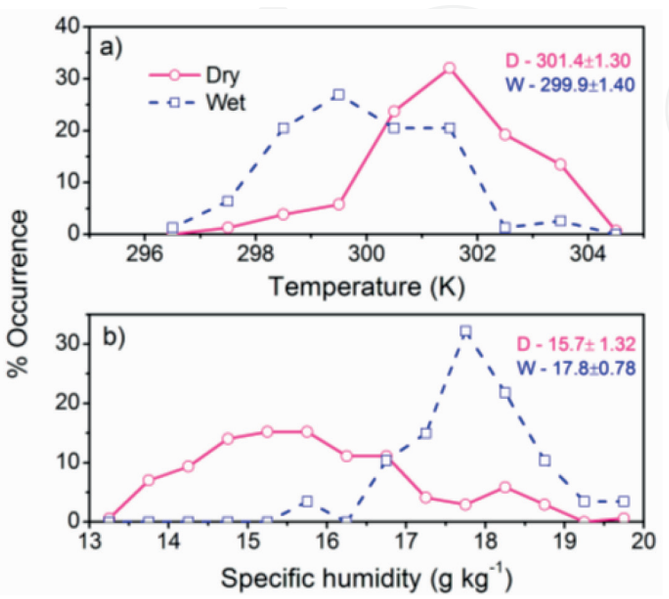

Figure 4.
Frequency distributions (in terms of % occurrence) for the surface (a) temperature and (b) humidity during wet and dry spells. The means of the distribution are also shown in the figure (source from [47]).

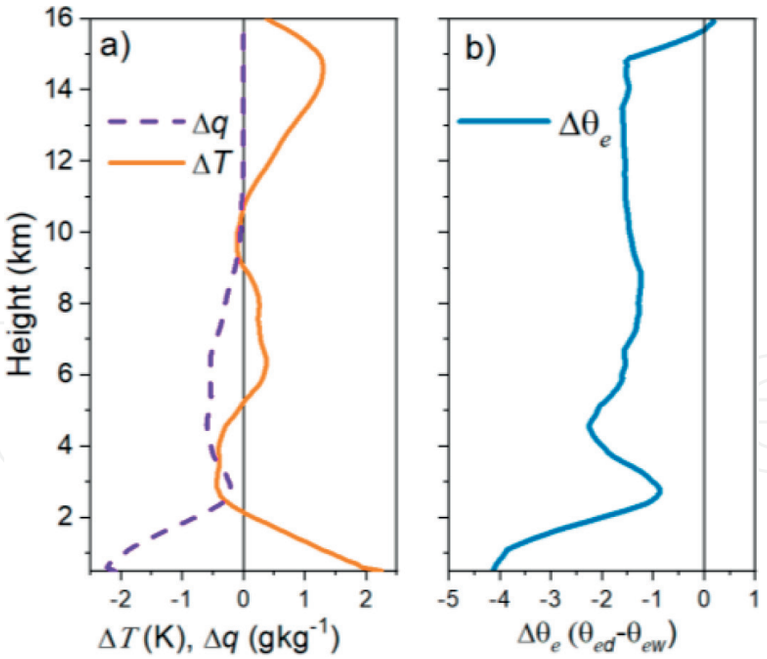

Figure 5.
Vertical profiles of (a) mean temperature, humidity and (b) equivalent potential temperature differences between wet and dry spells ($T = T_d - T_w$, $q = q_d - q_w$, and $\Delta\theta_e = \theta_{ed} - \theta_{ew}$). Suffixes 'd' and 'w' denote dry and wet spells, respectively (reproduced from [47]).

2 and 11 km, the temperature difference between spells is small (the temperature is higher in wet spell than in dry spell in two height regions, 2–5 and 9–10.7 km). The present observations do not show a clear heating in the middle troposphere during the wet spell, in contrast with the earlier studies during the wet spell of the Australian and Indian monsoon systems (over oceans) [34–36]. Similarly, the difference in q composites between wet and dry spells is relatively large below 7 km (>0.5 g kg^{-1}), except in the height region from 2 to 4 km, and small q in this height region is perhaps due to the enhanced detrainment and humidity in dry spell.

Except for this narrow layer, the results are consistent with those obtained in Australia and India, where a moist environment was observed over greater depths during the active phase of monsoon [34–36]. Yet, the role of advection in drying the troposphere during dry spells is not clear. Evaporation of surface moisture can explain the observed humidity differences between spells. Though there are no large local water bodies nearby, evaporation of surface moisture (in general is more during wet spell because of more rain) can enhance humidity in the lower troposphere, as observed in the figure, during wet spell. The other possible candidate for the dryness of the atmosphere during dry spells is large-scale subsidence from higher altitudes.

Next, several potential instability indices (stability index, CAPE, etc.) have been developed to measure the susceptibility of a given temperature and moisture profile to the occurrence of deep convection. Perhaps the most popular and widely used parcel instability parameter is CAPE. The variabilities of the different parcel instability parameters (CAPE, CINE, and stable layers) from wet to dry spells are primarily discussed. **Figure 6a–d** shows the frequency distributions of lifting condensation level (LCL), equilibrium level (EL), CAPE, and CIN during wet and dry spells. Quantitatively, about 71% (only 25%) of the LCL population is larger than 800 hPa during wet (dry) spell. The mean values of LCL for wet and dry spells are, respectively, 827 and 772 hPa. In contrast, EL distributions during wet and dry spells exhibit an opposite trend with cloud systems reaching higher altitudes in wet spells. Among the parcels which reached the EL, about 42 (11) %

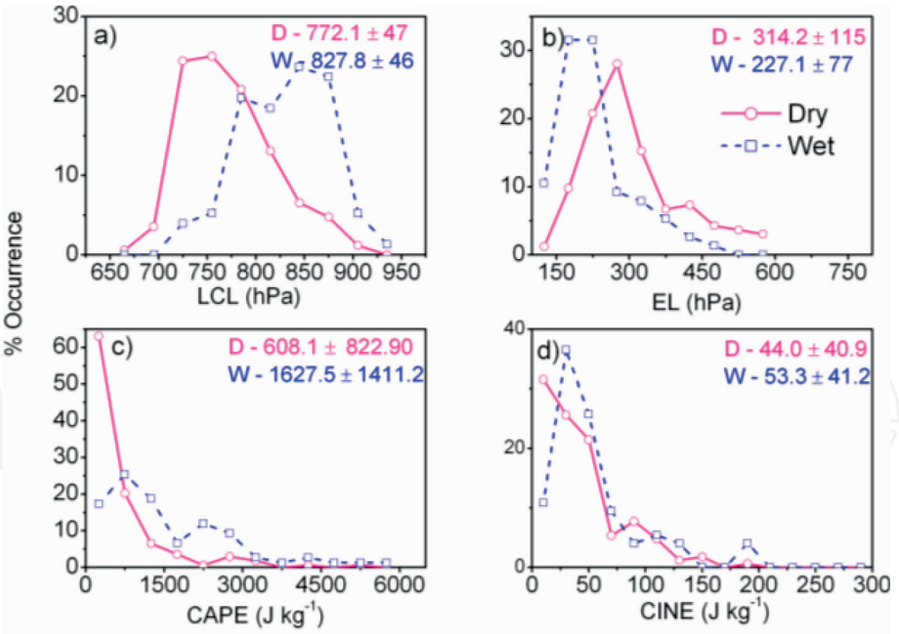

Figure 6.
Frequency distributions (in terms of % occurrence) for (a) LCL, (b) EL, (c) CAPE, and (d) CINE. The means of the distribution are also shown in the figure (source [47]).

of the EL population during wet (dry) spells shows values smaller than 200 hPa with mean altitudes of EL for wet (dry) spells being 227 (314) hPa. Distributions of LCL and EL altitudes indicate that clouds are deeper in wet spell than in dry spell. CAPE distribution and mean CAPE values are different in different spells with large values of CAPE which are seen more frequently in wet spell (**Figure 6**). For example, ~32 (6) % of the CAPE population in wet (dry) spells shows values larger than 2000 J kg^{-1}. Mean CAPE value for wet spells (1627 ± 1411 J kg^{-1}) is larger than for dry spells (608 ± 823 J kg^{-1}), and interestingly standard deviation of CAPE is also large in both spells. Note that the CAPE is estimated from the sounding data available at a fixed time, i.e., ~17:00 LT. Some of the soundings, therefore, represent conditions before active convection and some after convection and others at the time of convection. This perhaps is the main reason why we see significant variation in CAPE values within the spell. The distributions for CINE look similar in both spells (**Figure 6d**) with mean CINE nearly equal (53.3 ± 41.2 and 44 ± 41 J kg^{-1} for wet and dry spells, respectively). Like in the case of CAPE, in both spells, the variability within the spell is comparable to the mean value of CINE for that spell. The range of CINE observed at Gadanki is comparable to that observed over other tropical continental stations (Singapore 1.3 N, 103.8E, [37]) but smaller than that observed over oceans [38]. Although the mean values of CINE are small, they can be considerable on individual days. Note that the present observations were taken during the dusk hours, and therefore the second possibility can be ruled out. If we do not consider any forced lifting, an updraft of ~9 m s^{-1} is required to overcome CINE of ~40 J kg^{-1}. Existence of such strong vertical velocities in non-convective periods is rare. Therefore, in both spells, some external forcing is required to overcome this inhibition energy and to trigger convection.

Contrasting with other studies, CAPE values estimated over tropical oceans (Bay of Bengal and western Pacific) are in contrast to the present observations, with large values in break phase (before convection) and small in active phase [34, 38–40]. The regions influenced by maritime and continental flows also show similar features with larger values of CAPE in mesoscale convective systems associated with the break phase than those with active phase, for example, over Darwin in northern Australia [41] and over Brazil [42]. The main physical reason for the lower

values of CAPE in active spells is associated with the decrease of equivalent potential temperature (θe) due to the overturning of the atmosphere during convection [34]. This could be, during wet spell, convective downdrafts induced by precipitation loading, melting, and evaporation bring the relatively dry mid-tropospheric air into the boundary layer and reduces θe near the surface. In addition, the latent heat release in deep clouds warms the middle and upper troposphere and reduces the instability of the atmosphere. All these factors reduce the CAPE during active phase of the monsoon or during the convectively active period. However, at Gadanki, variation in thermodynamical parameters from wet to dry spells is greater near the surface and in the boundary layer. Above the boundary layer and in the middle troposphere (~2.5–11.5 km), the temperature difference between the composites for wet and dry spells is within 0.5 K. Also, in contrast to the expected, larger θe values are observed during wet spell in the lower troposphere [43].

Next, to examine the impact of stable layers in governing the convection growth, **Figure 7** shows the vertical distribution of stable layers in terms of lapse rates (top panel) and percentage occurrence (bottom panel). Following [47], the vertical distribution of % occurrence of temperature lapse rates exceeding certain thresholds (3, 4, and 5 K km^{-1}, all are smaller than the moist atmospheric lapse rate in the troposphere, ~6 K km^{-1}) during dry and wet spells are shown in **Figure 7a** and **b**. Following the procedure described by [47], the % occurrence of stable layers at each altitude is estimated from the ratio between the number of occurrences when the lapse rate exceeds a threshold and the total number of lapse rate data points at that altitude (see [47] for more details). From the analysis it was observed that statically stable layers are predominantly seen in the lower and middle troposphere (below 8 km). The % occurrence distribution for 5 K km^{-1} temperature lapse rate shows a

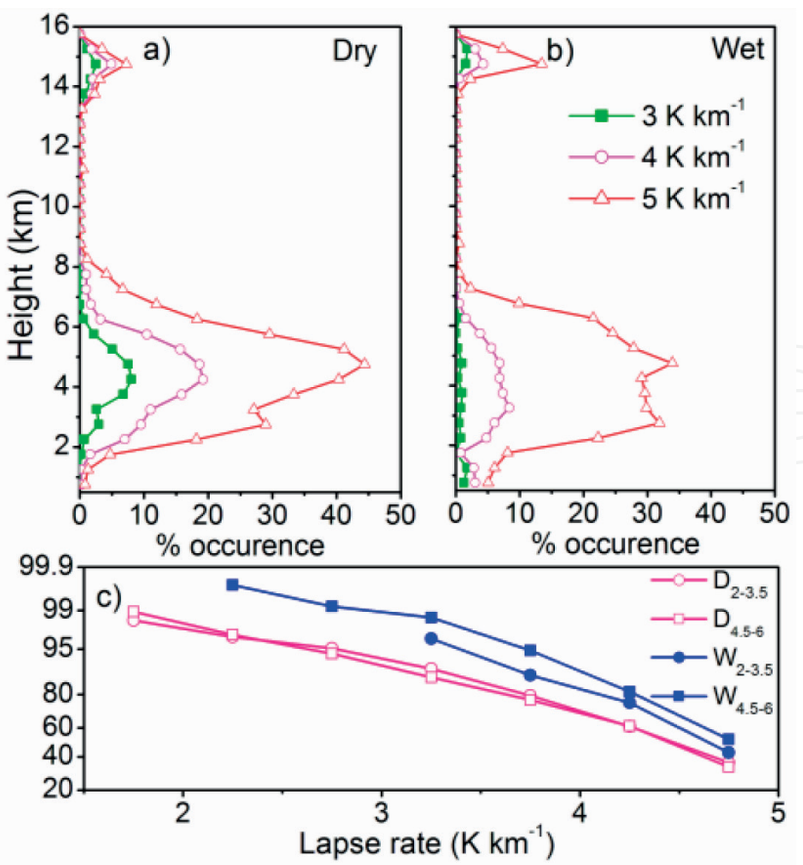

Figure 7.
Vertical distribution of % occurrence of stable layers defined by different temperature lapse rates during (a) dry and (b) wet spells. (c) Frequency distribution of temperature lapse rates during wet and dry spells in two height regions (2–3.5 and 4.5–6 km). D and W denote dry and wet spells, respectively (figure from [47]).

broad distribution between 2 and 7 km with two small peaks centered on 2–3 km and 5 km, while the distributions for other two temperature gradients show a single peak centered around 4.5 km in dry spell and slightly at a lower altitude in wet spell. Nevertheless, the magnitude of % occurrence is different in both spells. The peak in the height region of 2–3 km corresponds very well with the altitude of the boundary layer height and the second peak with the 0°C isotherm level. **Figure 7b** shows the cumulative distribution of the magnitude of stable layers in the height region of 2–3.5 and 4.5–6 km (the height regions in which the % occurrence of stable layers is relatively more) during dry and wet spells. Interestingly, both height regions exhibit strongest stable layers which exist in dry spell. Contrasting the lapse rate distributions in these two height regions indicates that gradients near the freezing level are stronger than their counterparts at low levels. This is true in both spells of the monsoon.

From **Figure** 7, strong inversion layers exist below 6 km height region during dry spell. These stable layers prohibit the growth of convection and modify the distribution of moisture. In other words, the stable layers will enhance the detrainment and thereby moisture near that level; Ref. [33] also supports this view based on draft core statistics. They observed that the shallow cores are more prevalent in dry spell with the maximum percentage occurrence of core tops in the height region of 3–5 km.

5.2 Energetics

In the earlier section, thermal characteristics of wet and dry spells are discussed at a tropical station, situated over southeastern peninsular India. Now, a logical question is raised, whether the observed feature of wet and dry spells is only confined to a station or extended throughout southeastern peninsular India. This issue is discussed in the following section.

For the estimation of CAPE and related thermal parameters, along with the observations, three global reanalysis products are utilized (ERA-interim; MERRA; and NCEP). For more details and description of the data sets (see [44–46]). Though all the gridded data sets were available at 00, 06, 12, and 18 UT, data at 12 UT were only employed, as it coincides with the balloon launch time over the stations.

Since variations in CAPE largely depend on parcel level of origin and its temperature and moisture content as discussed in above section, here, the exercise is repeated to compare with reanalysis products. **Figure 8** shows the composite percentage occurrence of moisture (q) and temperature (T) during wet and dry spells. Wet spells (dashed curves) are relatively moist and cooler than dry spells over Gadanki region, corroborating with [47]. Although the distribution of surface T and q in these spells exhibit reasonably good agreement among the reanalysis products, mean magnitudes differed by 2–3 K in T and ~2 g kg^{-1} in q. Further, a considerable difference between the percentage occurrence of sonde and reanalysis data products is noteworthy. From **Figure 8**, it is observed that surface parcels are more moist and cooler in the reanalysis products than observations, indicating the surface instability in reanalysis are larger than sonde observations. These large differences in the surface parcel thermal properties thus result in large differences in CAPE.

Next, atmospheric stability during wet and dry spells by means of q and T profiles over Gadanki is discussed. Vertical profile of q' over Gadanki from GPS radiosonde observations and reanalysis data are shown in **Figure 9a** and **b**. As expected, it is observed that wet spell q' composites are moist, with magnitudes reaching 1.5 g/kg, compared to dry spell. During dry spell, dryness in the atmosphere, as evidenced by negative q′, is extending throughout the tropospheric column below 100 hPa. However, more prominent drying is seen at two levels, one below 800 hPa level and

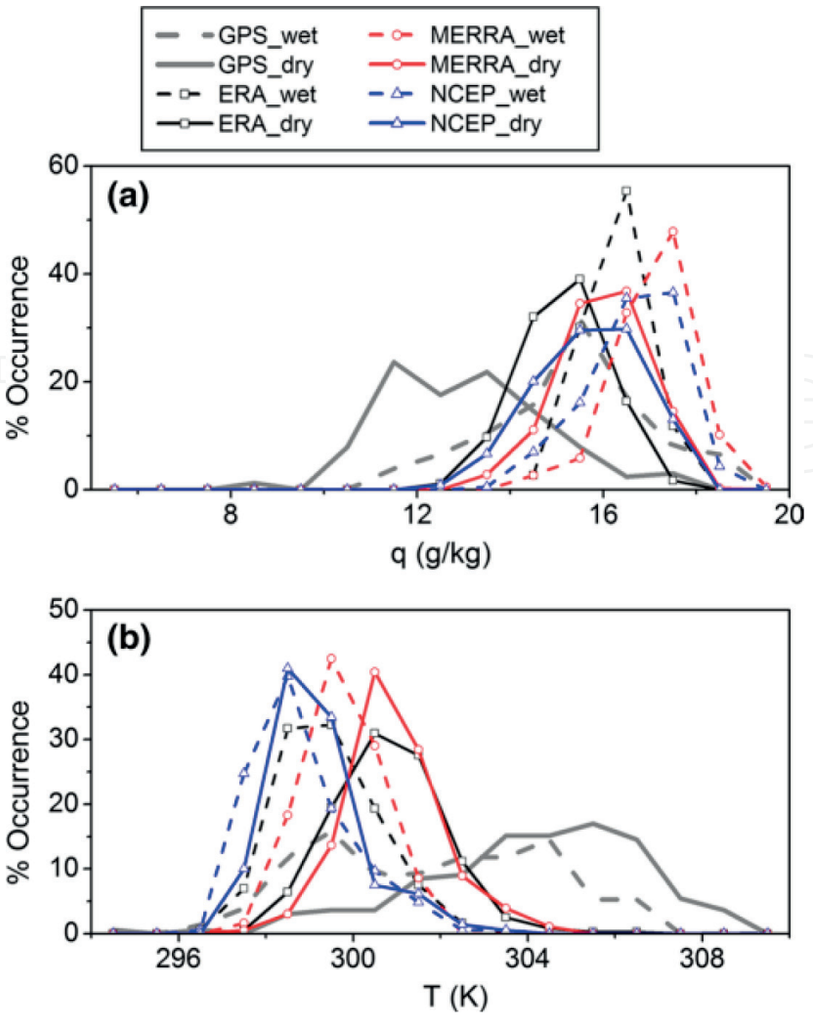

Figure 8.
Histogram of parcel moisture (a) and temperature (b) from GPS sonde observations and reanalysis products during dry (solid line) and wet (dashed line). Different colors in the legend represent the different products (source: [48]).

the other at upper tropospheric levels around 400–500 hPa. Although reanalysis data exhibit a good agreement with the observations, magnitudes of q anomalies slightly vary. For instance, upper tropospheric drying and moistening are not clearly visible in composite profiles of NCEP in both dry and wet spells. From **Figure 9**, it is inferred that changes in the T' are much smaller especially around mid-troposphere levels, with the magnitudes ranging from ±0.5 K in both the spells. However, large changes are seen only at boundary layer heights (below 800 hPa) spell composites (see **Figure 9c, d**). Vertical distribution of anomalous T depicts warmer (cooler) environment at lower (upper) levels over the study region, which represents the destabilization of the tropospheric lapse rate. In contrast, wet spell composite profile of T' exhibits cooling in the lower levels and slight warming (< 0.5 K) in the upper troposphere. This upper level warming and lower level cooling in T' are not confined to single station but rather observed all over SE peninsular India. Although the vertical profile patterns of T' are consistent with the observations, magnitudes differ at certain pressure levels especially around boundary layer heights. For instance, boundary layer warming and cooling are stronger in ERA (black curve) than NCEP (red curve). The differences in the magnitudes of T and q will have a profound effect on the buoyancy of the parcels and CAPE, which will be discussed next.

Figure 10 depicts the percentage occurrence of CAPE, during dry and wet spells computed from observations and reanalysis products. An obvious over estimation of CAPE by reanalysis data compared to observations in both spells is noticed, and the

values are more in MERRA and NCEP in dry spell and only in MERRA during wet spell, respectively. Although reanalysis products overestimate CAPE magnitude, they reproduce the differences in CAPE between spells reasonably well. Thus, it is clear from **Figure 10** that mean (or mode) of CAPE distribution is larger in wet spell than in dry spell. All reanalysis exhibits this feature, albeit with different magnitudes. For instance, difference between CAPE in wet and dry spells is nearly equal (~ 800 J kg^{-1}) when estimated with GPS and ERA-interim data. In contrast, NCEP- and MERRA-estimated mean CAPE values show smaller difference between spells (~250 J kg^{-1}

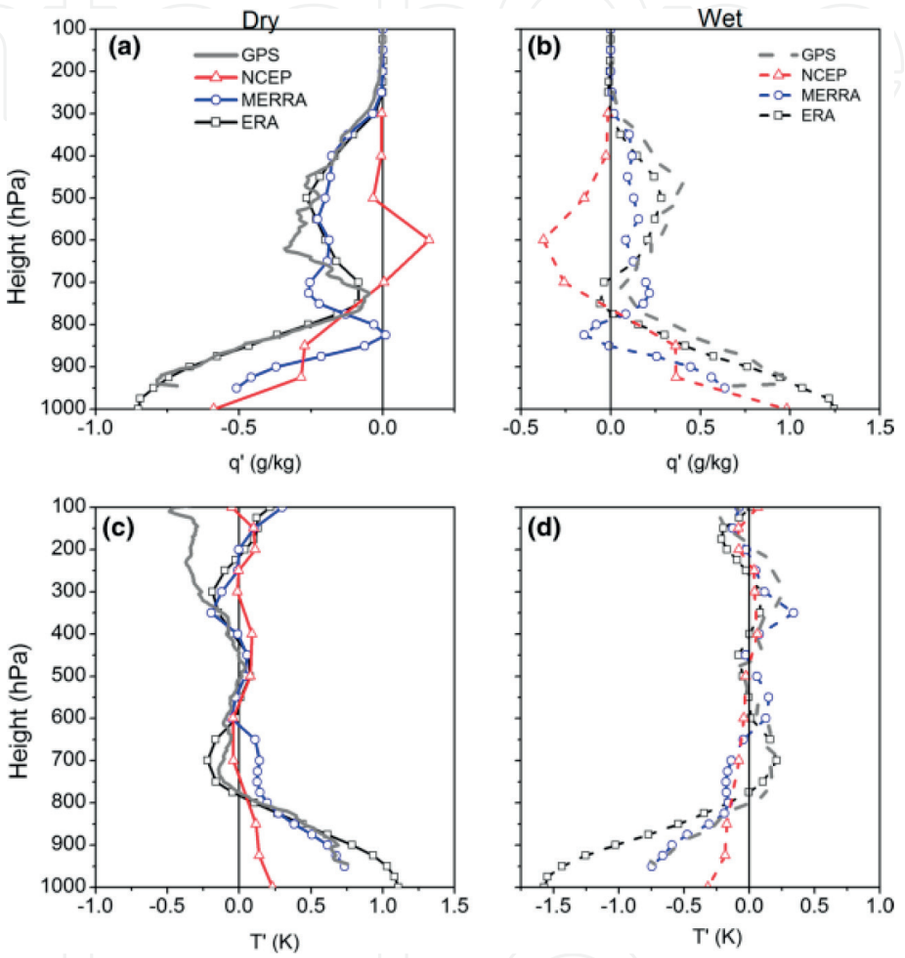

Figure 9.
Vertical profiles of anomalous moisture (a, b) and temperature (c, d) during dry and wet spells over Gadanki, from the sonde observations and reanalysis products (source [48]).

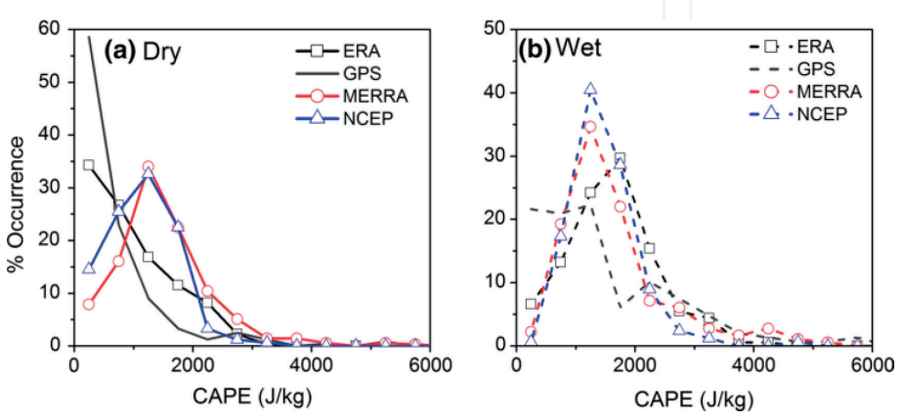

Figure 10.
Histograms of CAPE (at Gadanki) in (a) dry and (b) wet spells, respectively, as estimated by GPS sonde measurements and reanalysis outputs, illustrating the differences in CAPE between the spells (source [48]).

for NCEP and ~150 J kg^{-1} for MERRA). It is obvious from the above discussion that reanalysis products underestimate the CAPE variation within the spells when compared with sonde observations. Earlier, [34] have shown that while CAPE is strongly controlled by the properties of the boundary layer air, large positive buoyancy and realization of CAPE, however, occur above 600 hPa. Later, [47] also observed this feature over Gadanki using GPS radiosonde observations. Now, to examine how far reanalysis mimics this feature, parcel positive buoyancy area is divided into three layers (L1, 700–500 hPa; L2, 500–300 hPa; and L3, 300–200 hPa) to understand which positively buoyant layer is contributing more toward total CAPE in the spells. First, buoyancy for each layer is estimated from each sounding, and the contribution of each layer to total CAPE is estimated. These data are then grouped based on wet and dry spells, and the % occurrence for the layer contribution to total CAPE is estimated for each layer separately.

Figure 11 shows some intriguing similarities and differences in CAPE between spells, between layers, and between reanalysis and observations. In general, both reanalysis and observations show similar distribution of CAPE contributions by different positively buoyant layers. Among these layers, contribution of L2 to CAPE is more (~ 50%) in majority of the cases in both spells. From **Figure 11**, contribution of L1 to total CAPE is about ~38% (20–30%), and the remaining is by L3 in the wet (dry) spell. Also, the distribution in L1 during dry spell is relatively broader than in wet spell. Note that, for a few cases, the contribution of L1 (and to some extent L2) to CAPE is found to be as high as 100% in dry spell (**Figure 11a**), which indicates the vertical extent of clouds is limited in dry spell. This is consistent with report by [33] over Gadanki. All the reanalysis products reproduced above features; nevertheless, contributions of different positively buoyant layers to total CAPE are different. For example, the contribution of L3 to CAPE is relatively small in MERRA in wet spell. Although there are slight variations that exist in representation of

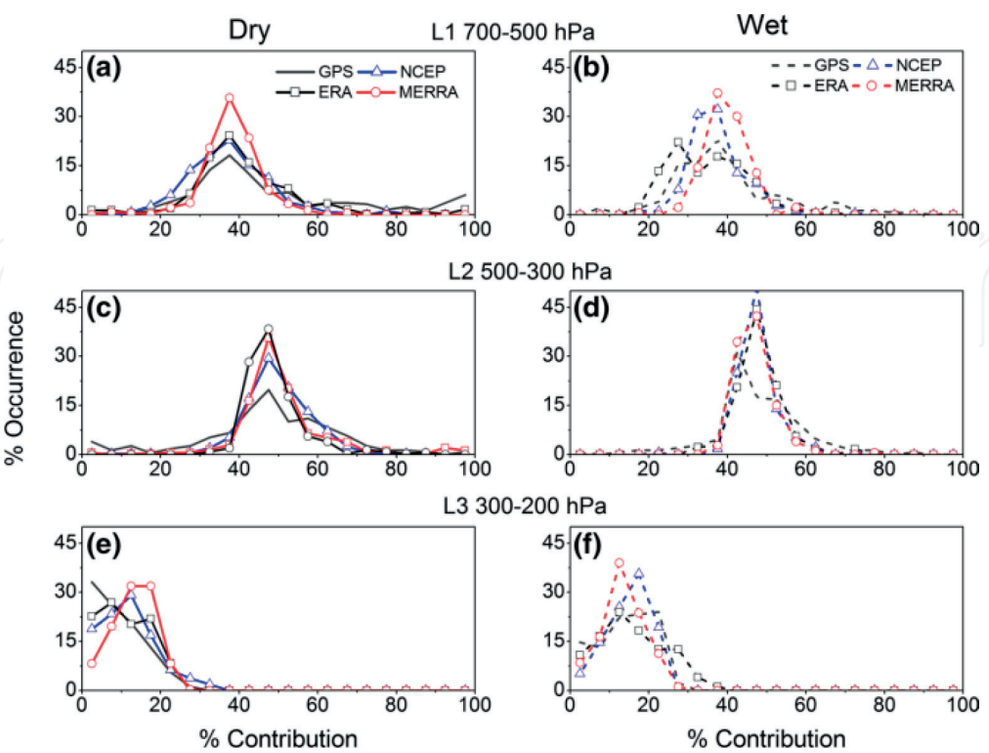

Figure 11.
Contribution of CAPE in different layers (L1: 700–500 hPa, L2: 500–300 hPa, L3: 300–200 hPa) to total CAPE in dry ((a), (c) and (e))wet ((b), (d) and (f)) spells at Gadanki. GPS sonde measurements and NCEP, ERA-interim, and MERRA reanalysis outputs are used in this analysis (source from [48]).

CAPE during the spells, it is clear from the analysis that ERA data reproduce similar CAPE variation between spells as obtained by radiosonde measurements.

Spatial variability of anomalous CAPE during wet and dry spells over SE peninsular India from the reanalysis products is shown in **Figure 12**. Note that, here, main focus is to find out the difference in dry (**Figure 12 (a)-(c)**) and wet (**Figure 12 (d)-(f)**) spells over SE peninsular India, and therefore, the analysis is restricted only to that region. It is clear from **Figure 12** that during wet spell, CAPE is larger in all the products [47]. These large CAPE values are not confined to single station but rather observed all over southeastern peninsular India. In contrast, negative CAPE values are seen during dry spell in all the reanalysis products. These −ve CAPE magnitudes, during dry spell, reconfirms that the thermal stability of the atmosphere during dry spell is significantly less for convection to trigger. Though there are similarities that exist among the reanalysis products, slight differences in magnitudes are noted especially during dry spell. For example, magnitudes of anomalous CAPE in MERRA are much less (~40 J kg^{-1}) than ERA (~200 J kg^{-1}). These differences are perhaps due to various convective parameterizations employed in the reanalysis products and also the vertical resolutions of the data products used.

Further, it is also noted from the buoyancy profiles during the spells that majority of positive buoyancy profiles show two peaks during dry spell and single upper tropospheric peak in wet spells at most of the grid points over southeast peninsular India (see Table 5 in [48]). Overall, majority of the buoyancy profiles, i.e., ~64%, exhibit bimodal distribution in dry spell, while single-peak buoyancy profiles are more prominent in wet spell (~56%), indicating the difference in the vertical distribution of parcel thermal buoyancy is not confined to single station but is a characteristic feature over the entire SE India. The analysis showed that, in this region, CAPE is higher in wet spell than in dry spell by ~1000 J kg^{-1}. Now it is imperative to understand the observed differences in CAPE between spells. In order to answer this, several plausible mechanisms are examined to explain the observed

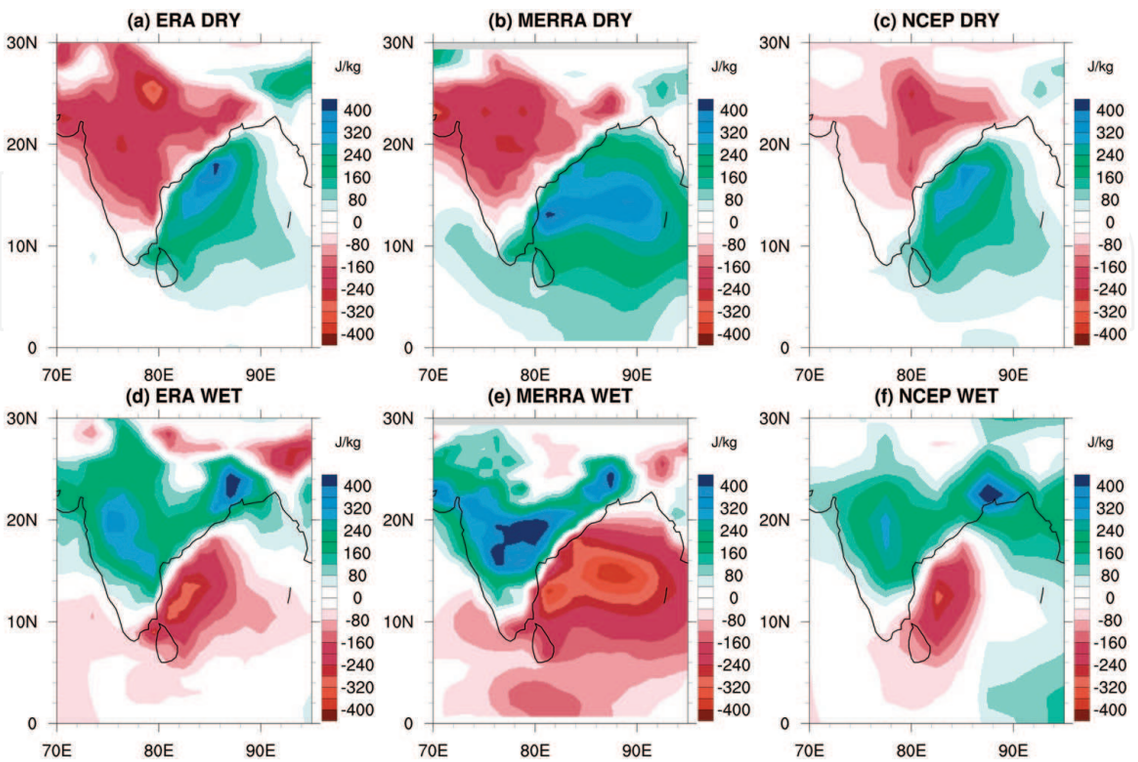

Figure 12.
Spatial distribution of anomalous CAPE in dry ((a)-(c)) dry and wet (d)-(f) spells, from three reanalysis products, over the southeast peninsular India (reproduced from the [48]).

CAPE differences between spells, i.e., time of sounding with respect to the rain occurrence, rapid rebuild-up of the instability, moistening of the atmosphere due to the evaporation of surface moisture in wet spell, enhanced low-level moisture convergence, enhanced downdrafts engendered by evaporative cooling, and drop dragging in dry spell. The weak CAPE in dry spell may not be sufficient to overshoot the frequent stable layers occurring in this spell. All these above mechanisms seem to be occurring in dry spell limiting the convection growth and CAPE [48].

5.3 Dynamical characteristics

In the previous sections characteristics of wet and dry spells are studied with respect to the thermodynamical point of view. The analysis reveals significant variability in surface moisture and temperature, vertical structure, and also CAPE between spells, which clearly indicates the thermal structure, available energy, and their forcing are different in spells over SE peninsular India. Therefore, one would expect differences in circulation features during wet and dry spells. Thus, in the present section differences in mean wind, vertical structure and diurnal variation with a special emphasis on monsoon quasi permanent systems (likes of LLJ and TEJ) over south eastern peninsular India are studied.

Majority of the data were obtained by collocated instruments available at Gadanki. Surface winds during the spells are measured from automatic weather station (AWS) along with Doppler sound detection and ranging (SODAR) wind components in the height region from 60 m to 1 km. Zonal and meridional winds above 1 km to upper troposphere (~18 km) are derived from low atmospheric wind profiler (LAWP) and Indian mesosphere-stratosphere and troposphere radar (IMSTR). Note that, although the instruments were not operated simultaneously as they were deployed in different years, it is believed that the mean winds represent the overall vertical structure and variability.

Figure 13 shows mean vertical profiles of mean wind and deviation during dry and wet spells of the monsoon over Gadanki. Since measurements utilized to generate this vertical wind structure by IMSTR, LAWP, SODAR, and AWS were not simultaneous, composite vertical profiles were not constructed. Rather, **Figure 13** shows average wind variation between spells in different altitude ranges (surface, obtained from AWS; 60 m to 1 km, obtained from SODAR; 600 m to 4 km, obtained from LAWP; and 3.6 to 19 km, obtained from IMSTR) [52].

Mean surface winds from AWS measurements (**Figure 13c**) during wet spells are relatively weaker than in dry spell, but the differences in zonal and meridional winds between the spells are not significant. However, the wind direction remained southwesterly in both spells. SODAR winds in the height region of 60 m–1 km remain northwesterly to westerly but exhibit large vertical variation in magnitude, particularly the zonal component. Zonal wind component attains their peak strength in the height region 200–500 m during both the spells, and in particular the intensity of zonal winds is stronger during dry spells (~4 ms^{-1}) than wet spell (<2 ms^{-1}), and further, the maximum difference between the spells is found in the height region of nocturnal low-level jet (NLLJ). In contrast, meridional winds are weak in amplitude (~1 ms^{-1}) during both the spells and do not show any significant differences between the spells. In the height regions from 600 m to 4 km, LAWP-derived winds continued to be westerly to northwesterly in both spells. The presence of LLJ is clearly seen in the zonal wind component, and interestingly, the height of LLJ peak varies during both spells (e.g., at 2.25 and 1.35 km in dry and wet spells, respectively). In addition, magnitude of the LLJ is also different with enhanced LLJ in the dry spell (16.8 ms^{-1}) than in wet spell (9.8 ms^{-1}). Interestingly, the difference in zonal wind between the spells is more pronounced above 1.5 km.

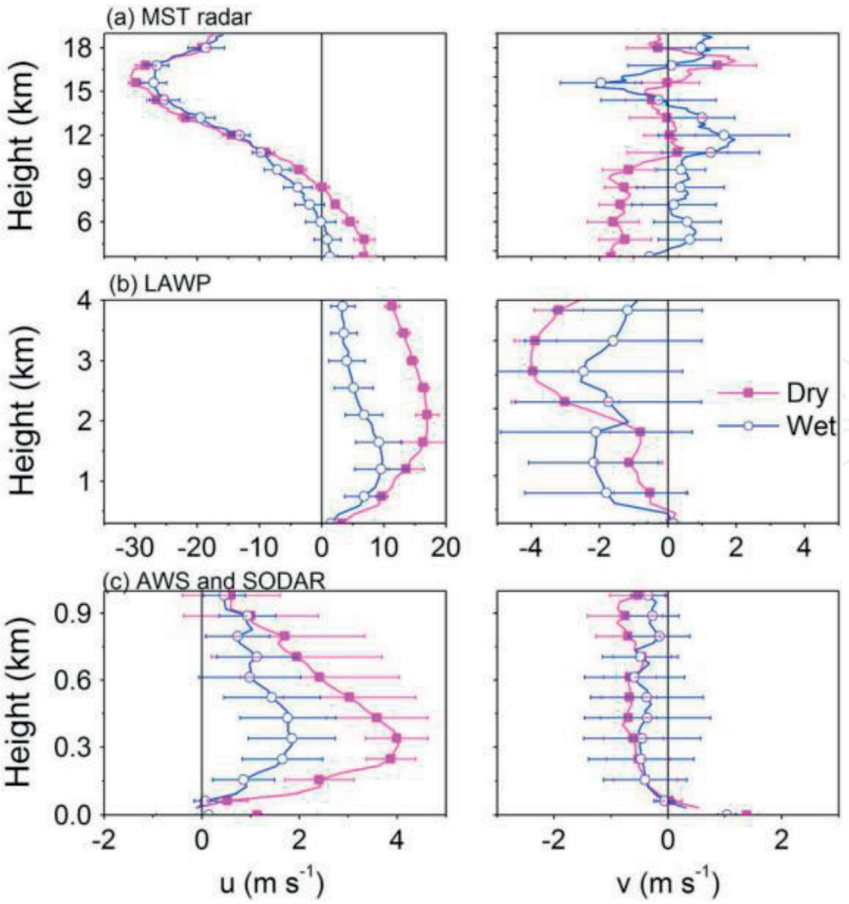

Figure 13.
Vertical profiles of (left column) zonal and (right column) meridional winds for wet and dry spells obtained from different instruments ((a) MST radar (1995–2013), (b) LAWP (1999–2000 and 2010–2011), and (c) SODAR (2007–2009) and AWS (2006–2013)). The average wind shown at 0 km (or surface) in ***Figure 13c*** *is obtained from AWS. Vertical profiles shown in* ***Figure 13a–c*** *are daily averages. The standard deviation is represented with error bars. Years in the brackets indicate data averaging periods (source from [52]).*

In contrary, the magnitude of meridional winds is relatively small and does not show significant variation between spells. IMSTR winds reveal that the vertical structure of wind in the height region of 3.6–19 km is different in both spells. There is a significant difference in vertical structure of winds from IMSTR, in the height region from 3.6 to 19 km, in both wet and dry spells (**Figure 13a**). These differences are pronounced in the lower and middle troposphere (below 8 km). The zonal wind profiles show typical summer monsoon circulation with low-level westerlies and strong upper tropospheric easterlies. Wind reversal height (i.e., from westerly to easterly), however, is different during both monsoon spells. The depth of westerlies is relatively shallow (deep) during the wet (dry) spell with zonal wind reversal occurring below 6 (8) km and then turns to easterly. On the other hand, the TEJ strength is found to be nearly the same in both spells with an average value of ~30 ms^{-1}. The height of the TEJ maximum is also found to be nearly the same during both spells (~16 km).

This section discusses the differences in the spatial variability of the jet streams between the spells. Composites of LLJ and TEJ for wet and dry spells and the wind anomaly (mean wind for dry spell-mean wind for wet spell) are estimated. Note that the main idea is to study the spatial variability of LLJ and TEJ when the monsoon convection is weak or active over southeast India. It allows us to examine the spatial extent of observed wind differences at Gadanki.

Figure 14 exhibits the spatial variation of mean zonal wind pattern for dry (**Figure 14a**) and wet (**Figure 14b**) spells and their difference (**Figure 14c**) on

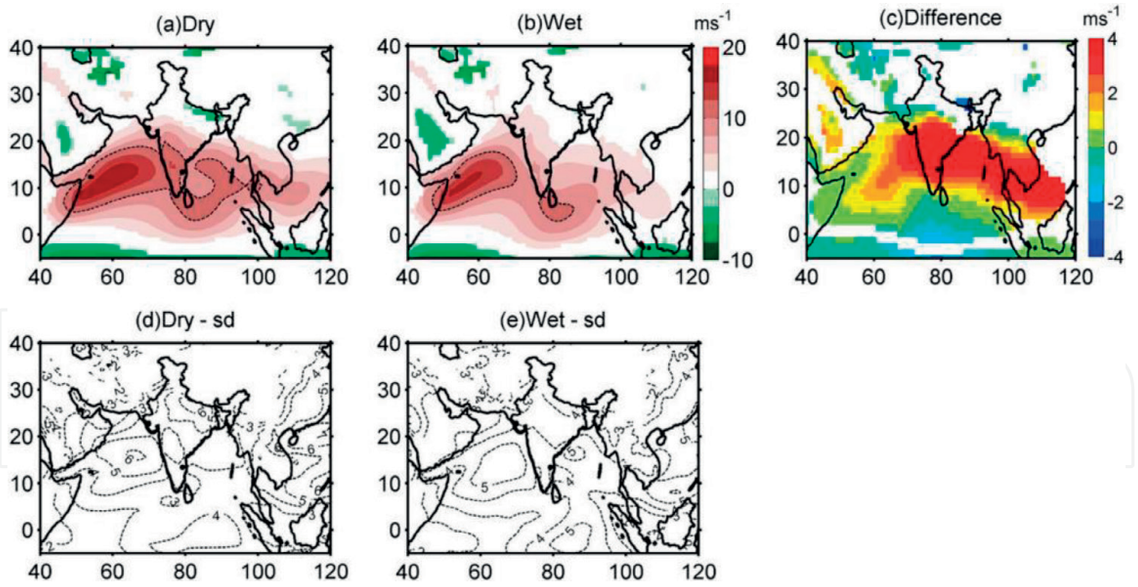

Figure 14.
Mean zonal wind on 850 hPa level from MERRA data for (a) dry and (b) wet spells, during 1995–2013, showing the spatial variation of LLJ. The black dashed line in ***Figure 4a*** *and* ***b*** *represents 10 ms^{-1} contour. (c) the difference in LLJ between spells (dry-wet). The dot denotes the location of Gadanki. (d and e) the spatial distribution of standard deviation of mean values for dry and wet spells, respectively (source from [52]).*

850 hPa level. Spatial distribution of the standard deviation of means for dry and wet spells is shown in **Figure 14d** and **e**, respectively. One commonality is the presence of LLJ in both the spells albeit with different magnitude and spatial distribution. During the dry spell (**Figure 14a**), the core of the LLJ splits over the Arabian Sea with one branch (say first branch) passing over the southern peninsular India centered around 16°N and the other toward southeast and veers cyclonically (second branch) before merging with the first branch in the Bay of Bengal (near the coast of Malay peninsula). On the other hand, only one branch (second branch) is present during the wet spell (**Figure 14b**). This splitting of LLJ in the Arabian Sea can be attributed to barotropic instability [49]. In this study, the splitting of LLJ is clearly evident during the dry spell (analogous to all-India active spell) [50, 51]. The presence of southward branch of LLJ during the break spell as reported by [48] is also seen here. In fact, this second branch is present in both spells with similar magnitude, as seen by the small wind anomaly present in that region (**Figure 14c**). **Figure 14c** clearly shows that large differences exist between the spells in LLJ magnitude and its spatial variation. A band of large positive wind anomaly passes over the Arabian Sea, Peninsular India, Bay of Bengal, and Malaysia with a maximum (~6 ms^{-1}) over the Southern Peninsular region. This large wind anomaly is significant and is occurring mainly due to the absence of first branch of LLJ during the wet spell. A negative anomaly in zonal wind is also observed in two regions, just south of the equator and near foot hills of the Himalayas. In general, the low-level westerly winds turn cyclonically in the North Bay of Bengal and become easterlies. These easterlies are clearly seen during the dry spell (or all-India active spell) (**Figure 14a**). As the monsoon trough moves northward to foot hills of the Himalayas during wet spell (or all-India break spell), the magnitude of easterlies became very weak (**Figure 14b**). In fact, the easterlies are completely absent over the Indian land-mass during the wet spell.

Spatial variation of mean zonal wind and standard deviation during wet and dry spells along with zonal wind difference between the spells at 100 hPa level is described in **Figure 15**. The easterly winds are strong in both spells and seen

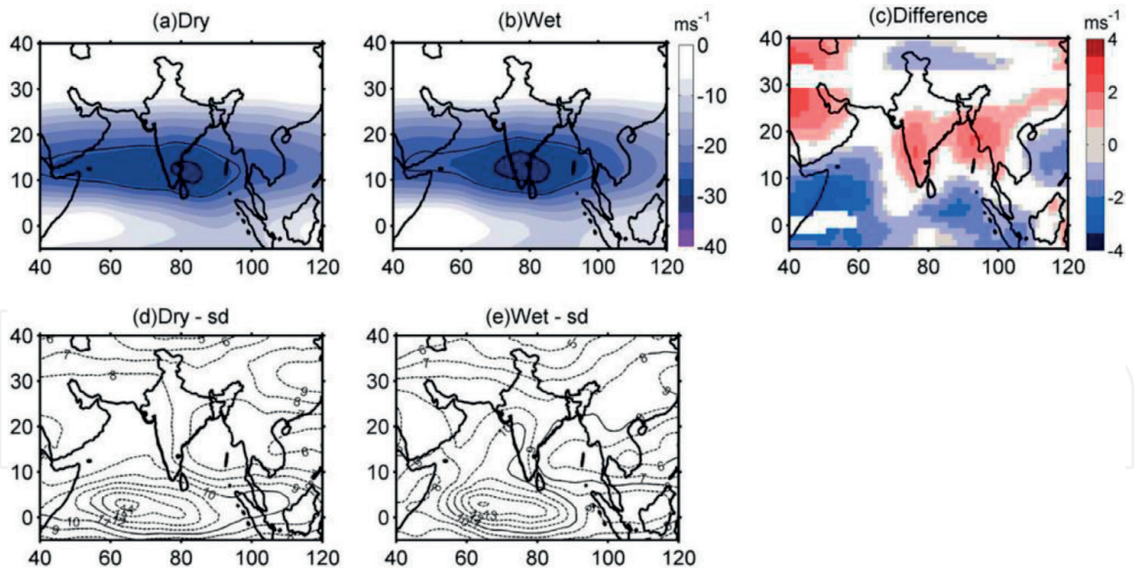

Figure 15.
*Same as **Figure 14** but for zonal winds at 100 hPa level, showing the TEJ variation. The black thin and thick solid lines in **Figure 15a** and **b** represent 24 and 28 ms^{-1} contours, respectively (source from [52]).*

prominently between 10°N and 20°N with winds as large as 30 ms^{-1} corroborating the radar observations made at Gadanki (**Figure 13a**). However, longitudinal extent of TEJ during dry spell is found to be more than in wet spell. It can be evidenced by 28 ms^{-1} (thick black solid line) and 26 ms^{-1} contour (thin black solid line) of TEJ. For instance, the 26 ms^{-1} contour is seen between the longitudes 40°E and 100°E during the dry spell, while it is only confined between 45 E and 95°E during the wet spell. Earlier, [49] observed a significant ISV in TEJ axis on 200 hPa level. They observed the axis of the TEJ along 15°N during the break spell, while a southward shift in the TEJ axis is observed during the active spell at 70°E. Such a north–south shift in TEJ axis is not observed in either of the spells here. The axis is found to be aligned along ~15°N latitude during both the spells.

6. Summary, conclusion, and discussion

Synthesis of spatial and vertical structures and regional characteristics of wet and dry spells over southeast peninsular India is presented in this chapter. In spite of its importance, not many reports exist on rainfall and its variation on different temporal scales over this region during southwest monsoon, partly because the rainfall in this region is relatively less, and it forms only a minor part of all-India rainfall (see **Figure 3a**). With the goal in mind, an attempt has been made to understand differences in thermal and dynamical characteristics and energetics of the atmosphere between wet and dry spells of the Indian summer monsoon over the southeast India. To better understand the aforementioned processes, data collected with a suite of unique instruments at NARL, model reanalysis data sets, and satellite rainfall products are effectively utilized.

It is observed that the difference in the thermal structure between wet and dry spells is significant only in the lower troposphere (<2–3 km). The distributions and mean CAPE values, which are measures of thermal instability, for wet and dry spells, are found to be different. Analysis indicates that mean CAPE in wet spell is found to be higher than that of in dry spell by ~1000 J kg^{-1}. The vertical extent of positive buoyancy profiles is deep during wet spells, while most of the buoyancy profiles during dry spells are limited in vertical extent. Further, the negative buoyancy areas are seen

in most of the profiles during dry spell, and they are mostly centered on two height regions, ~700 and ~500 hPa. They, probably, are due to the strong inversions and stable layers present at those altitudes. The convection growth is limited in dry spells due to the presence of strong stable layers, weak CAPE, and a relatively dry environment.

Reanalysis data products indicate CAPE is higher in wet spell than in dry spell over the entire southeast peninsular India. Majority of buoyancy profiles show only one peak during wet spell, while bimodal vertical distribution is seen predominantly in dry spell. From this analysis it is found that the differences in CAPE and buoyancy vertical structure between wet and dry spells are not only confined to Gadanki but rather observed all over southeastern peninsular India, and they are characteristic features of wet and dry spells. Several possible mechanisms are invoked to explain observed CAPE differences between spells, i.e., rapid rebuild-up of the instability, moistening of the atmosphere due to the evaporation of surface moisture in wet spell, enhanced downdrafts engendered by evaporative cooling, and drop dragging in dry spell. The synthesis of all measurements and estimates indicate that the observed weak CAPE in dry spell may not be sufficient to overshoot the frequent stable layers occurring in this spell. Further, the strong (magnitude) and deep (in height) low-level wind shear observed in dry spell seems to be shearing apart the weakly buoyant updraft.

Diurnal variation of winds from surface to the lower stratosphere is studied during different spells of the monsoon. It is observed that, over the study region, the surface and low-level mean winds are stronger during dry spells. The surface wind (both zonal and meridional) exhibits a clear diurnal cycle with strong (weak) wind during day (night) in both spells. Both the amplitude and time of wind maxima change with the altitude. For instance, the zonal wind maxima observed at noon near the surface is shifted to early morning in the height region of 400 m–1.5 km (1 km) and then systematically to evening (noon) in the height region of 3–6 km (1–2.5 km) in dry (wet) spell. The depth of westerlies is deeper in dry spell than in wet spell. Also, the zonal wind reversal height shows clear diurnal variation in wet spell, while it is nearly the same in dry spell. The amplitude of the diurnal cycle increases with altitude up to 2 km and then decreases. Largest amplitudes of the diurnal cycle (>8 m s^{-1}) are found in the height region of 1–2 km. The splitting of LLJ into two branches over the Arabian Sea is quite pronounced in dry spell, with one branch passing over the peninsular India and the other branch veering cyclonically and joins the first branch in the Bay of Bengal. The strength and the axis of TEJ do not vary much between spells. These variations are compared and contrasted with earlier reports on jet streams.

The diagnostics made with the in situ observations and reanalysis products and the key results obtained can be exploited for the modeling purpose for better prediction of subseasonal variability of rainfall regionally.

Acknowledgements

The author would like to thank the director of the National Atmospheric Research Laboratory, Gadanki, for providing necessary facilities to carry out the work. The author would also like to thank Dr. T. Narayana Rao, NARL, for providing critical comment and helpful discussion in shaping out this work.

Acronyms

ITCZ	intertropical convergence zone
TCZ	tropical convergence zone

ISV	intraseasonal variability
ISMR	Indian summer monsoon rainfall
ISO	intraseasonal oscillation
IMD	India Meteorological Department
NARL	National Atmospheric Research Laboratory
MSL	mean sea level
GMT	Greenwich mean time
AWS	automatic weather station
CAPE	convective available potential energy
CINE	convective inhibition energy
LCL	lifting condensation level
LFC	level of free convection
EL	equilibrium level
ERA	European Center for Medium Range Weather Forecasting reanalysis
NCEP	National Center for Environmental Prediction
MERRA	Modern Era Retrospective analysis for Research and Applications
LLJ	Low-level jet
TEJ	tropical easterly jet
IMSTR	Indian mesosphere-troposphere stratosphere radar
LAWP	low atmospheric wind profiler
SODAR	sound detection and ranging

Author details

Mohana S. Thota
Department of Civil Infrastructure and Environmental Engineering,
Khalifa University, Abu Dhabi, United Arab Emirates

*Address all correspondence to: drmohanthota@gmail.com

References

[1] Ramage CS. Monsoon Meteorology (International Geophysics Series). Vol. 15. San Diego, California: Academic Press; 1971. 296 pp

[2] Slingo. Monsoon: Overview. UK: University of Reading, Elsevier Science Ltd.; 2003

[3] Pai DS, Rajeevan M. Summer monsoon onset over Kerala: New definition and prediction. Journal of Earth System Science. 2009;**118**:123-135

[4] Gadgil S, Kumar KR. The Asian monsoon—Agriculture and economy. In: Wang B, editor. The Asian Monsoon. Berlin: Springer; 2006. pp. 651-683

[5] Sikka DR, Gadgil S. On the maximum cloud zone and the ITCZ over Indian longitude during southwest monsoon. Monthly Weather Review. 1980;**108**:1840-1853

[6] Goswami BN, Ajay Mohan RS. Intra-seasonal oscillations and interannual variability of the Indian summer monsoon. Journal of Climate. 2001;**14**:1180-1198

[7] Goswami BN, Ajaymohan RS, Xavier PK, Sen gupta D. Clustering of synoptic activity by Indian summer monsoon intraseasonal oscillations. Geophysical Research Letters. 2003;**30**:1431. DOI: doi 10.1029/2002GL016734

[8] Jones C, Waliser DE, Lau WKM, Stern W. The Madden-Julian oscillation and its impact on northern hemisphere weather predictability. Monthly Weather Review. 2004a;**132**:1462-1471

[9] Singh SV, Kripalani RH. The south to north progression of rainfall anomalies across India during the summer monsoon season. Pure and Applied Geophysics. 1985;**123**:624-637

[10] Singh SV, Kripalani RH. Application of EEOF analysis to interrelationships and sequential evolutions of monsoon fields. Monthly Weather Review. 1986;**114**:1603-1610

[11] Singh SV, Kripalani RH. Low frequency intra-seasonal oscillation in Indian rainfall and outgoing long-wave radiation. Mausam. 1990;**41**:217-222

[12] Kripalani RH, Singh SV, Arkin PA. Large-scale features of rainfall and outgoing long-wave radiation over Indian and adjoining regions. Contributions to Atmospheric Physics. 1991;**64**:159-168

[13] Kriplani RH, Kulkarni A, Singh SV. Association of the Indian summer monsoon with the northern hemisphere midlatitude circulation. International Journal of Climatology. 1997;**17**:1055-1067

[14] Kulkarni A, Sabade SS, Kriplani RH. Spatial variability of intra-seasonal oscillations during extreme Indian monsoons. International Journal of Climatology. 2009;**29**:1945-1955

[15] Webster PJ, Magana VO, Palmer TN, Shukla J, Tomas RA. Monsoons: Processes, predictability, and the prospects for prediction. Journal of Geophysical Research. 1998;**103**:4451-4510

[16] Gadgil S. The Indian monsoon and its variability. Annual Review of Earth and Planetary Sciences. 2003;**31**:429-467

[17] Rajeevan M, Bhate J, Kale JD, Lal B. High resolution daily gridded rainfall data for the Indian region: Analysis of break and active monsoon spells. Current Science. 2006;**91**:296-306

[18] Swaminathan MS. Abnormal monsoon and economic consequences:

The Indian experience. In: Fein JS, Stephens PL, editors. Monsoons. Washington, D.C: John Wiley & Sons; 1987. pp. 121-133

[19] Parthasarathy B, Munot AA, Kothawale DR. Regression model for estimation of Indian food grain production from summer monsoon rainfall. Agricultural and Forest Meteorology. 1988;**42**:167-182

[20] Gadgil S, Abrol YP, Seshagiri Rao PR. On growth and fluctuation of Indian food grain production. Current Science. 1999a;**76**:548-556

[21] Abrol IP. India's agriculture scenario. In: Abrol YP, Gadgil S, Pant GB, editors. Climate Variability and Agriculture. New Delhi: Narosa Publishing House; 1996. pp. 19-25

[22] Blanford HF. Rainfall of India. Monsoon Monograph—India Meteorological Department. 1886;**2**:217-448

[23] Ramamurthy K. Monsoon of India: Some aspects of the 'break' in the Indian southwest monsoon during July and August. Forecasting Manual, India Meteorological Department, Pune, India. 1969;**18**(3-IV):1-57

[24] Magna V, Webster PJ. Atmospheric circulations during active and break periods of the Asian monsoon. In: Preprints of the Eighth Conference on the Global Ocean-Atmosphere-Land System (GOALS). Atlanta, GA: Amer. Meteorol. Soc.; 1996

[25] De US, Lele RR, Natu JC. Breaks in southwest monsoon. Report No. 1998/3. New Delhi, India: India Meteorological Department; 1998

[26] Krishnan P, Kunhikrishnan PK, Nair SM, Ravindran S, Jain AR, Kozu T. Atmospheric boundary layer observations over Gadanki using lower atmospheric wind profiler-preliminary results. Current Science. 2003;**85**:75-79

[27] Gadgil S, Joseph PV. On the breaks of the Indian monsoon. Proceedings of the Indian Academy of Sciences - Earth & Planetary Sciences. 2003;**112**:529-558

[28] Ramesh Kumar MR, Desai P, Uma R. A new criterion for identifying breaks in monsoon conditions over Indian subcontinent. Geophysical Research Letters. 2004;**31**:L18201. DOI: 10.1029/2004GL020787

[29] Prasad VS, Hayashi T. Large-scale summer monsoon rainfall over India and its relation to 850 hPa wind shear. Hydrological Processes. 2007;**21**:1992-1996

[30] Klingaman NP, Weller H, Slingo JM, Innes PM. The intraseasonal variability of the Indian summer monsoon using TMI sea surface temperatures and ECMWF reanalysis. International Journal of Climatology. 2008;**21**:2519-2539

[31] Krishnamurthy V, Shukla J. Intraseasonal and interannual variability of rainfall over India. Journal of Climate. 2000;**13**:4366-4377

[32] Rajeevan M, Gadgil S, Bhate J. Active and break spells of the Indian summer monsoon. Journal of Earth System Science. 2010;**119**:229-247

[33] Rao TN, Uma KN, Satyanarayana TM, Rao DN. Differences in draft core statistics from wet spell to dry spell over Gadanki (13.5° N, 79.2° E), India. Monthly Weather Review. 2009;**137**:4293-4306

[34] McBride JL, Frank WM. Relationships between stability and monsoon convection. Journal of the Atmospheric Sciences. 1999;**56**:24-36

[35] Bhat GS, Chakraborty A, Nanjundiah RS, Srinivasan J. Vertical thermal structure of the active and weak phases of convection over the north Bay of Bengal: Observation and model results. Current Science. 2002;**83**:296-302

[36] Webster PJ et al. The JASMINE pilot study. Bulletin of the American Meteorological Society. 2002;**83**:1603-1630

[37] Yi L, Lim H. Comparison of convective environments in tropical and extratropical atmospheres with 1989-2002 radiosonde data. In: 26th Conference on Hurricanes and Tropical Meteorology. AMS; 2004. pp. 1-71

[38] Bhat GS et al. BOBMEX: The Bay of Bengal monsoon experiment. Bulletin of the American Meteorological Society. 2001;**82**:2217-2243

[39] Mapes BE, Houze RA Jr. An integrated view of the1987 Australian monsoon and its mesoscale convective systems. Part I: Horizontal structure. Quarterly Journal of the Royal Meteorological Society. 1992;**118**:927-963

[40] Williams E, Renno N. An analysis of conditional instability of the tropical atmosphere. Monthly Weather Review. 1993;**121**:21-36

[41] Cifelli R, Rutledge SA. Vertical motion, diabatic heating, and rainfall characteristics in N. Australia convective systems. Quarterly Journal of the Royal Meteorological Society. 1998;**124**:1133-1162

[42] Halverson JB, Rickenbach T, Roy B, Pierce H, Williams E. Environmental characteristics of convective systems during TRMM-LBA. Monthly Weather Review. 2002;**139**:1493 1493-1493 1509

[43] Johnson RH, Ciesielski PE, Hart KA. Tropical inversions near the 0 °C level. Journal of the Atmospheric Sciences. 1996;**53**:1838-1855

[44] Dee DP, Uppala SM, Simmons AJ, Berrisford P, Poli P, Kobayashi S, et al. The ERA-interim reanalysis: Configuration and performance of the data assimilation system. Quarterly Journal of the Royal Meteorological Society. 2011;**137**(656):553-597

[45] Kalney E et al. The NCEP-NCAR 40-year reanalysis project. Bulletin of the American Meteorological Society. 1996;**77**:437-471

[46] Rienecker MM, Suarez MJ, Gelaro R, Todling R, Bacmeister J, Liu E, et al. MERRA: NASA's modern-era retrospective analysis for research and applications. Journal of Climate. 2011;**24**:3624-3648. DOI: 10.1175/JCLI-D-11-00015.1

[47] Mohan TS, Rao TN. Variability of the thermal structure of the atmosphere during wet and dry spells over Southeast India and its implication on draft cores. Quarterly Journal of the Royal Meteorological Society. 2012;**138**:1839-1851

[48] Mohan TS, Rao TN, Rajeevan M. Differences in CAPE between wet and dry spells of the monsoon over the southeastern peninsular India. Meteorology and Atmospheric Physics. 2018. DOI: 10.1007/s00703-018-0590-9

[49] Findlater J. Mean monthly airflow at low-levels over the western Indian Ocean. Geophysical Memoirs. 1971;**16**:1-53

[50] Joseph PV, Sijikumar S. Intraseasonal variability of the low-level jet stream of the Asian summer monsoon. Journal of Climate. 2004;**17**:1449-1458

[51] Sathiyamoorthy V, Pal PK, Joshi PC. Intraseasonal variability of the tropical easterly jet. Meteorology and Atmospheric Physics. 2007. DOI: 10.1007/s00703-006-0214-7

[52] Mohan TS, Rao TN. Differences in mean wind and its diurnal variations between wet and dry spells of the monsoon over southeast peninsular India. Journal of Geophysical Research. 2016. DOI: 10.1002/2015JD024704